

# fDOT Imaging of Vascular Autoregulation: Characterization Of Sensitivity, and Effect of Noisy Data

H.L. Graber<sup>1,2</sup>, M. Farber<sup>2</sup>, D. Sreedharan<sup>2</sup>, Y. Pei<sup>1</sup>, Y. Xu<sup>1,2</sup>, G.T. Voelbel<sup>3</sup>, G. Wylie<sup>3</sup>, J. Lengenfelder<sup>3</sup>, J. DeLuca<sup>3</sup>, R.L. Barbour<sup>1,2</sup>

<sup>1</sup>NIRx Medical Technologies LLC / 15 Cherry Lane, Glen Head, NY 11545; [hgrab@nirx.net](mailto:hgrab@nirx.net)

<sup>2</sup>Department of Pathology / SUNY Downstate Medical Center / 450 Clarkson Avenue, Brooklyn, NY 11203

<sup>3</sup>Kessler Medical Rehabilitation Research and Education Center / 1199 Pleasant Valley Way, W. Orange, NJ 07052



## INTRODUCTION

- A recently developed feature extraction procedure for functional diffuse optical tomography (fDOT) measurements involves computation of **autoregulatory state (AS)** information from time series of oxyhemoglobin ( $Hb_{oxy}$ ) and deoxyhemoglobin ( $Hb_{deoxy}$ ) images (Figure 1). [219 M-AM, 218 M-PM]
- An important objective is to use the AS approach to increase the amount and quality of relevant information derived from fDOT brain imaging studies. [229 M-AM, 145 W-AM]
- Before results of AS computations can be accepted with confidence, it is necessary to characterize the method's performance under expected levels of signal amplitude and noise.
  - How frequently do false-positive and false-negative findings occur?
- Tests of the AS method's reliability were conducted, using three classes of data:
  - Mathematical simulations: noise-free, noise-added, and pure-noise models
  - fDOT measurements performed on an inert tissue-simulating phantom
  - fDOT measurements collected from a human forearm (Figure 2) or human frontal cortex (Figure 3).
- Principles of physiology lead us to expect that any specified location in tissue should cycle through the autoregulatory states in the sequence indicated in Figure 1: 1→2→3→4→5→6→1...
- Transitions in the opposite direction, or in steps larger than one unit, should be rare.

Figure 1

Hemoglobin State	State 1	State 2	State 3	State 4	State 5	State 6
$Hb_{oxy}$	-	-	-	+	+	+
$Hb_{deoxy}$	-	+	+	+	-	-
$Hb_{total}$	-	-	+	+	+	-
Oxygen Balance	Balanced	Uncomp. Oxygen debt	Comp. Oxygen debt	Balanced	Uncomp. Oxygen excess	Comp. Oxygen excess
Favorable Transitions	→					
Unfavorable Transitions	←					

Figure 2



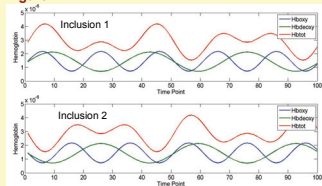
Figure 3



## METHODS

- Data types
  - Simulation
    - Noise-free
      - Medium is a geometric model of the human frontal lobe
      - Fluctuating levels of  $Hb_{oxy}$  and  $Hb_{deoxy}$ , as shown in Figure 4, are modeled in two pre-selected regions. [218 M-PM]
      - Elsewhere, composition of the medium is constant in time.
      - Measurements are computed by solving a diffusion-based light propagation equation.
    - Noise-added
      - Preceding results are modified, by adding Gaussian white noise to all computed measurement values.
      - Realistic noise model: magnitude increases with increasing distance between illuminating and detecting optodes (Figure 3).
    - Pure-Noise
      - Random numbers (Gaussian distribution) are used as the measurement data.
      - Image reconstruction algorithm uses measurements performed at two wavelengths. Correlation coefficient between the random number sequences used as dual-wavelength data was 0 (no correlation) in one case, and 0.9 (positive correlation) in another.
  - Tissue and laboratory-phantom measurements
    - Multi-channel continuous wave near infrared imaging (NIRx Medical Technologies).
    - Simultaneous dual-wavelength measurement with near infrared light (760nm and 830nm).
    - Forearm: 24 source and 24 detector optodes (576 channels; see Fig. 2). Brain: 30 source and 30 detector optodes (900 channels; see Fig. 3). Phantom: 32 source and 32 detector optodes (1024 channels, geometry similar to Fig. 2).

Figure 4



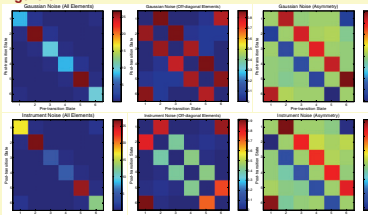
## Data Analysis

- Optical data low-pass filtered and normalized to a resting-baseline mean value.
- Images of  $\Delta Hb_{oxy}$  and  $\Delta Hb_{deoxy}$  concentrations computed by using a first-order perturbation algorithm.
  - $\Delta Hb_{oxy} = Hb_{oxy} - Hb_{oxy, baseline}$ ,  $\Delta Hb_{deoxy} = Hb_{deoxy} - Hb_{deoxy, baseline}$ .
- Six vascular autoregulatory states are defined, as shown in Figure 1, according to the algebraic signs of  $\Delta Hb_{oxy}$ ,  $\Delta Hb_{deoxy}$ , and their sum  $\Delta Hb_{total} = \Delta Hb_{oxy} + \Delta Hb_{deoxy}$ .
- Each relational category reasonably corresponds to a different underlying state of oxygen supply/demand balance or imbalance.
- Time fraction analysis:
  - Autoregulatory state calculation (Figure 1) allows us to compute not only the state-dependent  $\Delta Hb_{oxy}$  and  $\Delta Hb_{deoxy}$  concentrations, but also:
    - The percentage of image pixels that are in each state, at any time frame.
    - The percentage of overall time that each pixel spends in any of the six states.

## RESULTS

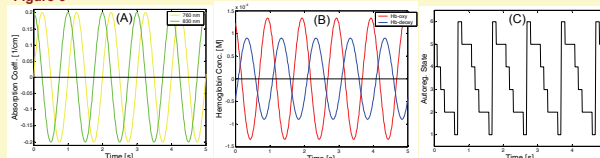
- Results of pure-noise simulation and laboratory phantom measurement
  - An autoregulatory state (AS) value was computed, for each image pixel and time frame, from the reconstructed  $\Delta Hb_{oxy}$ ,  $\Delta Hb_{deoxy}$  images.
  - The numbers of transitions, from one time frame to the next, between all AS pairs was counted
  - Results displayed as a 6x6 matrix, shown in Fig. 5.
  - Elements on the main diagonal (i.e., no transition occurs) dominate, so these are replaced with zeros to allow visualization of the off-diagonal elements
  - Difference between the transition matrix and its transpose reveals that physiologically unfavorable transitions occur more often than favorable ones, for the non-biological media considered here.
  - Explanation for preceding phenomenon hinges on the formulas used to recover  $\Delta Hb_{oxy}$  and  $\Delta Hb_{deoxy}$  from the two-wavelength measurement data.
    - The computation of Hb concentrations transforms uncorrelated dual-wavelength absorption data into negatively correlated  $\Delta Hb_{oxy}$ ,  $\Delta Hb_{deoxy}$  time series (Figure 6).
    - The resulting AS computation has two notable characteristics, seen for all noise-dominated data:
      - A preponderance of states 2 and 5 in the AS data.
      - Tendency for AS transitions to go in the "wrong" direction.
  - Consequently, if the physiologically expected trend is actually seen, it is almost certainly a real effect.
    - It is the opposite of what occurs by chance.

Figure 5



## RESULTS (cont.)

Figure 6



Legend: (A) Uncorrelated input data (e.g., tissue absorption coefficients at two wavelengths) yield  $Hb_{oxy}$  and  $Hb_{deoxy}$  time series, (B), that are strongly anti-correlated while the  $Hb_{total}$  signal has the larger amplitude. Consequently, states 2 and 5 are over-represented in the AS computation, and the transitions proceed in the opposite direction of the physiology-driven cycle.

- Model-based simulations (noise-free, noise-added):
  - Autoregulatory state (AS) can be determined exactly, for each inclusion region and time frame (Fig. 3, 4).
  - Ideal AS transition matrix shows preponderance of balanced states (1 and 4), which also is typical for resting tissue [Figure 7(A),(B)]
    - Owing to the simplicity of the modeled hemodynamics, transition matrix is nearly symmetric.
  - When images are reconstructed from noise-free data, a nearly perfect recovery of the original AS transition matrix is achieved [Figure 7(C),(D)]. [218 M-PM]
  - However, if the noise magnitude is excessive (i.e., noise SD = 30% of the noise-free detector reading), the pattern obtained resembles that for the pure-noise case [Figure 7(E),(F)].

- Forearm imaging results:
  - Inflation and subsequent rapid deflation of blood-pressure cuff (Fig. 2) produces profound physiological changes (Figure 8).
  - Cuff ischemia, wherein  $Hb_{oxy}$  falls and  $Hb_{deoxy}$  increases, to a significant extent.
  - Reactive hyperemia, where  $Hb_{oxy}$  overshoots its pre-inflation original baseline value and gradually recovers, and  $Hb_{deoxy}$  exhibits a corresponding "undershoot."

- We use this as a physiological positive control case.
  - Predicted AS cycling behavior must be observed here, if there is to be any possibility to seeing it in fDOT brain imaging data, where the hemodynamic fluctuations are much smaller.
  - In terms of both magnitude and spatial extent.
- Results of AS computations show the expected temporal sequence during reactive hyperemia, in both the spatial mean time series (Figure 9) and the individual image pixels' data (Figure 10).

Figure 7

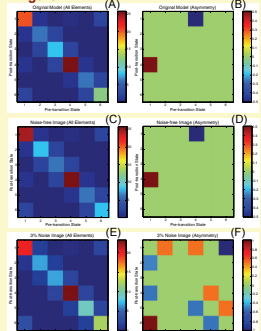


Figure 8

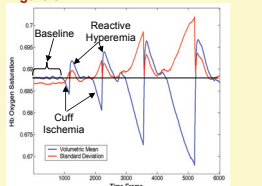


Figure 9

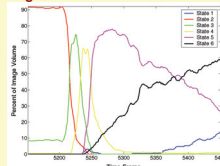
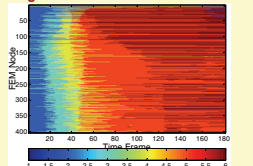


Figure 10



- The AS transition matrix has the structure predicted for physiological data, cycling through the states in the favorable order (Figure 11).
  - This result indicates that the image data have a structure qualitatively different from that of the synthetic or the laboratory phantom data.
  - Confirms that strongly ordered, non-random behavior is being recorded in the fDOT measurement data.
- In addition, the AS transition matrix for data collected during the resting baseline time interval (i.e., prior to the induced provocations) also exhibits a preponderance of transitions in the forward or favorable direction (Figure 12).
  - Thus it is reasonable to expect that the AS analysis approach will yield biologically meaningful and accurate results when applied to fDOT brain imaging data.
- Comparison of reactive hyperemia (Fig. 11) and baseline (Fig. 12) results also shows a significant difference:
  - Oxygen-excess states (5 and 6) predominate in the former condition, and balanced states (1 and 4) in the latter.
  - This is the result predicted, by reasoning from first principles of vascular physiology.

Figure 11

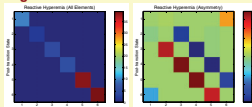
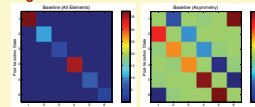


Figure 12



- Brain imaging results:
  - AS analysis applied to a selected participant in a clinical study, wherein verbal fluency tests were administered while fDOT measurements were collected over the frontal cortex (Figure 3).
  - Transition matrices are shown for both the 3-Back (Figure 13) and resting baseline (Figure 14) time intervals.

- Results parallel those obtained from the forearm experiment.
  - Forward/favorable direction cycling through the autoregulatory states predominates in both time intervals.
  - Balanced states predominate in resting baseline, and the fraction oxygen-excess states increases (but do not predominate) during performance of the task.
- Magnitudes of the various effects are smaller than in the forearm case.
  - Unsurprising, as the magnitude and spatial extent of the hemodynamic perturbations are much lower.

Figure 13

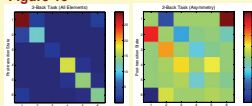
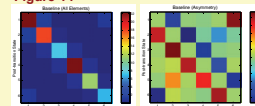


Figure 14



## CONCLUSIONS

- Autoregulatory-state analysis, when applied to data that are not of biological origin, produces results qualitatively different from the forearm and brain fDOT imaging studies.
  - This finding implies that high confidence can be placed in the results of AS analysis applied to physiological data: observed favorable-direction transitions are almost certainly genuine.
- The preceding, plus the magnitude of the effects obtained from the brain imaging data, indicate that proceeding to clinical research studies is justified, with presently available technology and data analysis capabilities.

## ACKNOWLEDGMENTS

Funded by the National Institute of Neurological Disorders and Stroke (KMRREC: 1F32 NS055509-01 and R41 NS050007; NIRx: R41 NS050007-01), and by the Henry H. Kessler Foundation (KMRREC).